

## Chapter 7

# Forward detectors

In addition to the main ATLAS detector systems described in the previous chapters, three smaller sets of detectors are being built to provide good coverage in the very forward region [213].

Ordered according to their distance from the interaction point as shown in figure 7.1, the first system is a Cerenkov detector called LUCID (LUMinosity measurement using Cerenkov Integrating Detector, see section 7.1). LUCID is the main relative luminosity monitor in ATLAS and is located at a distance of  $\pm 17$  m from the interaction point, near the TAS (Target Absorber Secondaries) collimator. The second system is the Zero-Degree Calorimeter (ZDC), located at a distance of  $\pm 140$  m from the interaction point (see section 7.3). This corresponds to the location where the LHC beam-pipe is divided into two separate pipes. The ZDC is embedded in the TAN (Target Absorber Neutral), located between the beam-pipes just after the split. The ZDC's primary purpose is to detect forward neutrons in heavy-ion collisions. The most remote detector is the absolute luminosity detector ALFA (Absolute Luminosity For ATLAS, see section 7.2). ALFA consists of scintillating-fibre trackers located inside Roman pots at a distance of approximately  $\pm 240$  m from the interaction point. Additional proton-tagging detectors are being considered at an even greater distance of about  $\pm 420$  m [214] from the interaction point. These detectors, together with new radiation hard-detectors at  $\pm 220$  m [215] are part of a possible upgrade programme.

### 7.1 The LUCID detector

Luminosity can be measured by several detectors in ATLAS, but LUCID (LUMinosity measurement using Cerenkov Integrating Detector) [213] will be the only detector which is primarily dedicated to online luminosity monitoring. LUCID is a relative luminosity detector. Its main purpose is to detect inelastic  $p$ - $p$  scattering in the forward direction, in order to both measure the integrated luminosity and to provide online monitoring of the instantaneous luminosity and beam conditions. Potentially, LUCID could also be used for diffractive studies, for example as a rapidity-gap veto or as a tag for a diffractive signal [216].

During the initial period of LHC operation, the absolute calibration procedure for LUCID will use calculations based on LHC machine parameters, initially determining luminosity to a precision of  $\sim 20 - 30\%$ . Physics processes can also be used, such as W and Z counting [217] and exclusive muon pair production via two-photon interactions [218]. The most accurate calibration will be

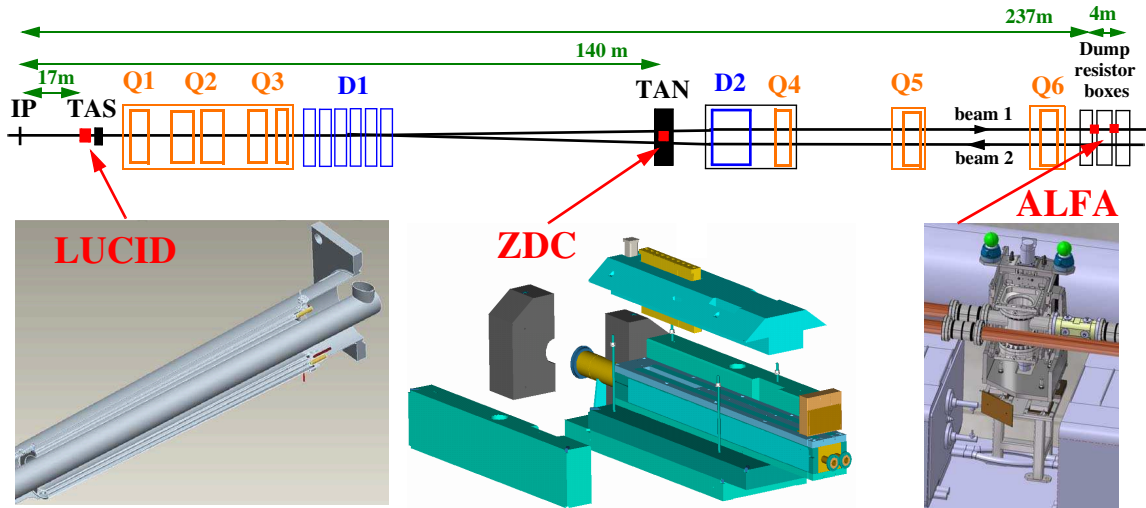


**Figure 7.1:** Placement of the forward detectors along the beam-line around the ATLAS interaction point (IP). See text for details.

obtained with the ALFA detectors which measure elastic Coulomb scattering. The goal is thus to measure the luminosity with an uncertainty of better than 5%.

At the LHC design luminosity, most bunch-crossings will result in multiple  $p$ - $p$  interactions. The number of interactions per beam-crossing must be known in order to determine luminosity. LUCID is based on the principle that the number of interactions in a bunch-crossing is proportional to the number of particles detected in this detector. This holds true even when most of the detected particles originate from secondary interactions.

The main requirements for the LUCID detector are:

- good acceptance for minimum-bias events;
- sufficient time resolution to measure individual bunch-crossings which occur every 25 ns;
- resistance to very high radiation levels;
- the ability to count individual charged particles;
- pointing capability in order to suppress signals from tracks which do not point to the interaction point.

The concept of a luminosity detector consisting of an array of Cerenkov tubes (cones) was developed by the CDF collaboration [219]. The main challenges in using this type of detector at the LHC are the much higher radiation and background levels. ATLAS has approved the construction of a detector with a reduced number of readout channels for the initial low-luminosity phase of the LHC operation (up to few  $10^{33} \text{ cm}^{-2} \text{ s}^{-1}$ ), with a view to then possibly upgrade the detector to a larger coverage if it can be demonstrated through further studies that the detector would work well at the LHC design luminosity.

Since there is no Landau tail in the measurement of Cerenkov light, it is in principle possible to determine the number of particles which have entered a Cerenkov tube by using pulse-height

measurements (particle-counting mode). The probability that several particles enter the same tube is quite low for the LUCID design, typically a few percent at a luminosity of  $\sim 10^{33} \text{ cm}^{-2} \text{ s}^{-1}$ . Simulations show that a simpler measurement consisting in counting only the number of tubes with a signal above a preset threshold (hit-counting mode) provides a measurement for online monitoring with an acceptable systematic error. These measurements will be done with different scalers for each bunch in the LHC, so that the luminosity of the individual bunches can be monitored online. A pre-scaled LUCID trigger will make it possible to record a sub-set of the LUCID events for offline analysis which may be done in particle-counting mode and thereby obtaining a more precise luminosity determination using charge and time-to-digital converters.

### 7.1.1 Detector design

The LUCID detector is depicted in figure 7.2. It consists of twenty aluminium tubes which surround the beam-pipe and point toward the interaction point. The 1.5 m long mechanically polished tubes with a diameter of 15 mm are placed in a light-weight aluminium gas vessel which ensures that the tubes are filled with  $\text{C}_4\text{F}_{10}$  at a constant pressure of 1.2–1.4 bar, providing a Cerenkov threshold of 2.8 GeV for pions and 10 MeV for electrons. There are two detectors installed, one in each end-cap region of ATLAS, at a distance of approximately  $\pm 17 \text{ m}$  from the interaction point, and placed at a radial distance of approximately 10 cm from the beam-line ( $|\eta| \approx 5.8$ ).

The Cerenkov light emitted by a particle traversing the tube has a half-angle of  $3^\circ$  and is reflected on average three times before the light is measured by photomultiplier tubes (PMT's) which match the size of the Cerenkov tubes. The signal amplitude from these PMT's can be used to distinguish the number of particles per tube, and the fast timing response provides unambiguous measurements of individual bunch-crossings. LUCID is situated in a high radiation area and, although the PMT's have quartz windows and are radiation hard, their performance is expected to degrade after several years of operation at nominal LHC luminosity. It is therefore foreseen to upgrade the detector after some years of operation. The Cerenkov light from the upgraded detector could be transmitted through radiation-hard quartz fibres to a region outside the forward shielding (see figure 3.1) with a low level of background radiation, in which the fibres would be read out with multi-anode PMT's. In this readout scheme, a Winston cone at the end of each Cerenkov tube focuses the light onto a bundle of 37 fused silica fibres with 0.8 mm diameter. A Winston cone is a parabola of revolution profile designed to maximise the collection of incoming rays. In order to gain experience with this type of readout, four of the twenty Cerenkov tubes are read out by fibres in this manner. The initial LUCID detector will not have a re-circulating gas system as it is not expected to be needed for the low-luminosity phase of the LHC. However, such a system could be envisaged for high-luminosity operations, should it prove to be necessary.

The 16 electrical signals from the PMT readout are fed into a custom-designed front-end card containing a fast amplifier and a differential line-driver. These analogue signals pass through a constant-fraction discriminator, which registers a hit each time the PMT pulse height is above a preset threshold. A charge-to-digital converter allows offline analysis of the signal amplitudes in a sub-sample of the triggered events. One of the digital outputs of the front-end card is fed into a multi-hit time-to-digital converter for offline timing analysis, with a second output going to a custom-designed 9U VME readout card. The readout card houses FPGA's used to calculate

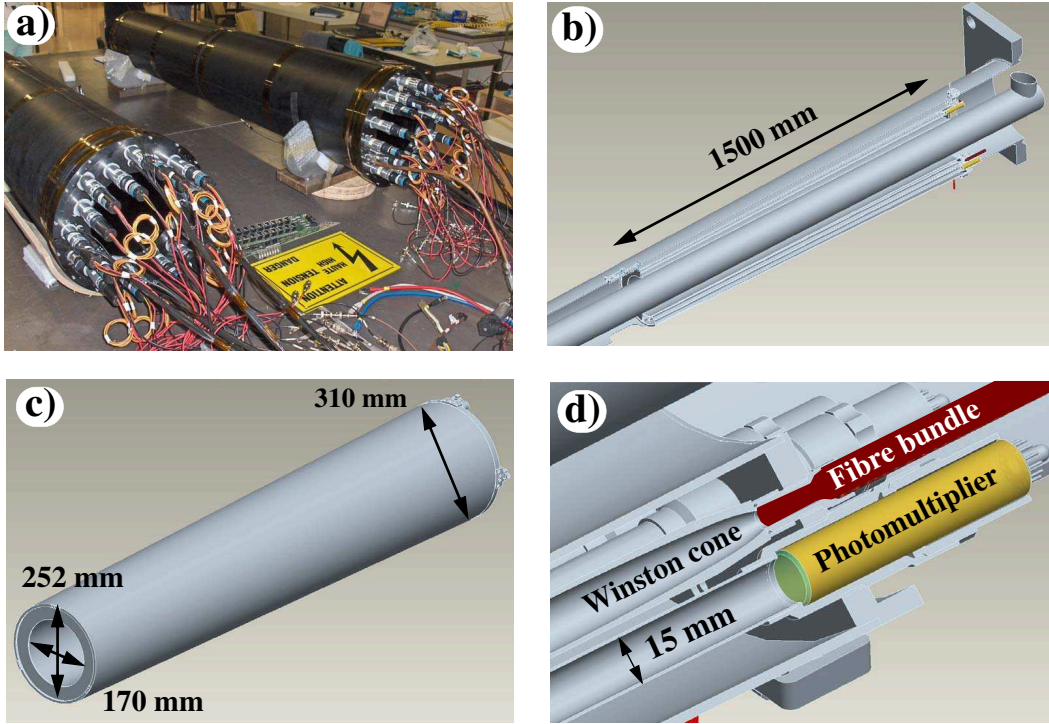


**Figure 7.2:** a) Picture of the two LUCID vessels fully assembled and ready to be installed in ATLAS. b) Sketch of LUCID integrated in the cone supporting the beam-pipe. c) Design of the gas vessel. d) Expanded view of the readout area showing the coupling between the 15 mm diameter Cerenkov tubes and the photomultiplier tubes. Also shown is the coupling between the Cerenkov tubes and the readout fibre bundle through a Winston cone (see text).

the luminosity for each bunch-crossing using different algorithms and stores one scaler value per bunch-crossing per luminosity algorithm. It is thus at the core of the LUCID online processing: after receiving a L1 trigger accept signal, it sends the pattern of hits to the overall readout system. It also provides an independent LUCID trigger. The LUCID readout buffer is sent to the trigger and data acquisition system via the S-link interface for inclusion in the overall event record.

### 7.1.2 Experimental results from test-beam and radiation tests

A six-tube prototype detector, dedicated purely to test-beam measurements, has been validated at DESY. The prototype was used to study the light-collection efficiency of both readout schemes, either with PMT's directly connected to the Cerenkov tubes or with bundles of optical fibres coupled to Winston cones attached to the Cerenkov tubes. The light output was studied as a function of angle, track position in the tube, pressure, Cerenkov-tube polish, PMT type, fibre type, number of fibres, and of the Winston cone design parameters. Figure 7.3 (left) shows an example of the number of photoelectrons collected in the PMT, when the Cerenkov tube was placed in a coaxial electron beam with an energy of 6 GeV. This test was performed using a Cerenkov tube with

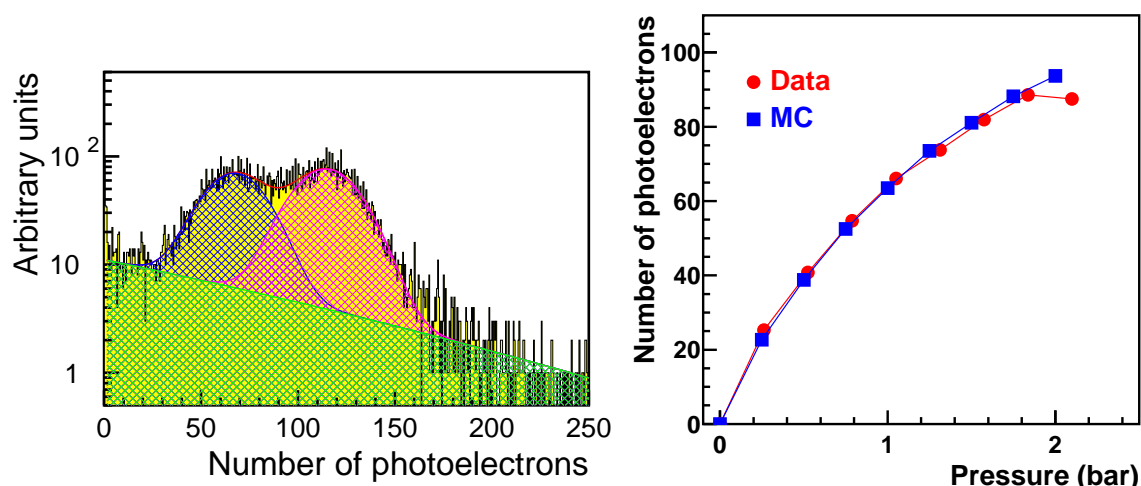


**Figure 7.3:** Left: distribution of the number of photoelectrons for an aluminised mylar Cerenkov tube as obtained at the electron test facility at DESY. The peak coming from the Cerenkov light in the radiator gas alone (left peak) and the one produced by the radiator gas and the quartz window of the readout PMT (right peak) are clearly visible. The curves superimposed on the experimental data represent the results of the fit with two gaussian distributions for the signal plus a linearly decreasing shape for the background. Right: comparison of the photoelectron yield from the Cerenkov light in the radiator gas as a function of the radiator gas pressure for the test-beam data (red circles) and Monte Carlo data (blue squares).

a larger diameter than the PMT window resulting in two peaks depending on whether the beam particles missed the PMT window or went through it. On average, Cerenkov light produced in the gas yielded about 70 photoelectrons and light produced in the PMT window about 50 photoelectrons. These values are being determined from test-beams for each tube and will be used to set their thresholds. Measurements also showed that the collected light yield drops off significantly for a tube-axis rotation greater than  $0.5^\circ$  with respect to a beam aligned with the tube axis. One of the main objectives of the test-beam measurements was to validate the GEANT4-based Monte Carlo [220] simulations of the detector. Figure 7.3 (right) shows a comparison of a measurement of the average number of photoelectrons as a function of radiator gas pressure with the simulated detector response. The agreement observed shows that the light collection is correctly simulated.

The radiation hardness of the detector and its readout is an important issue, although for the initial operation of the LHC, the total dose per year seen by LUCID will be less than one tenth of the dose at design luminosity (7 mrad per year). The body of the detector is made of aluminium and is extremely radiation hard. However damage to other components may be a concern (for instance, the PMT's, the optical fibres, the signal cables, the power cables and certain seals and bonds in the detector which were made using epoxy). Radiation testing of these components has been performed using both a strong gamma source and a reactor. So far, no serious problems have been observed in any of the materials tested.

### 7.1.3 LUCID installation in ATLAS

The LUCID detector is fully assembled and mechanically tested for gas leaks and light tightness. The front-end and readout scheme has been validated in the beam test at DESY. The calibration using LED light injected into each Cerenkov tube has been successfully tested in the fully assembled detectors. The detector is ready to be installed together with the beam-pipe in 2008.

## 7.2 The ALFA detector

Traditionally, the absolute luminosity at hadron colliders has been determined via elastic scattering at small angles. This is also the approach pursued by ATLAS with the ALFA (Absolute Luminosity For ATLAS) [213] detector. The optical theorem connects the elastic-scattering amplitude in the forward direction to the total cross-section and can be used to extract luminosity. In addition, other interesting physics topics may be explored with such scattering data [221].

The extremely small scattering angles ( $3 \mu\text{rad}$ ) needed to make these measurements are smaller than the nominal beam divergence. These measurements can therefore only be performed with specially prepared beam conditions, which are also used for calibration of the LUCID detector. High-beta ( $\beta^*$ ) optics in combination with reduced beam emittance are required. Moreover the detectors have to be placed far away from the interaction point and as close as possible to the beam. The Roman-pot technique has been successfully used in the past [222] for measurements very close to circulating beams and has therefore been adopted for ATLAS. The Roman-pot concept is based upon a detector volume (the pot) that is separated from the vacuum of the accelerator by a thin window but is connected with bellows to the beam-pipe and thus can be moved close to the beam. The ATLAS Roman pots have been designed to move the detectors as close as 1 mm to the beam, but only from above and below, due to the mechanical constraints imposed by the two horizontal beam-pipes of the LHC, as shown in figure 7.4. The Roman pots will be located  $\pm 240$  m away from the interaction point, and on each side there will be two Roman-pot stations separated by four metres.

The main requirements on the detectors which will be housed in the Roman pots are: a spatial resolution of about  $30 \mu\text{m}$ , no significant inactive edge region, minimal sensitivity to the radio-frequency noise from the LHC beams and compatibility with the vacuum in the Roman pots.

Given these requirements, ATLAS has chosen a scintillating-fibre tracker. The high- $\beta^*$  operation of the LHC corresponds to a very low instantaneous luminosity, and for this reason no radiation-hard technology is required for this specific set of detectors. Prototypes of the ALFA detectors have been validated in beam tests at DESY [223] and CERN [224]. In order to fulfil the spatial resolution requirements, the detector is built of ten double-sided modules, each with 64 fibres arranged in stereo  $u-v$  geometry on both sides. The square fibres have a width of  $0.5 \text{ mm}$ . The effective area of the detector is somewhat smaller than the  $32 \times 32 \text{ mm}^2$  due to the way the fibres are cut close to the beam (see figure 7.5). The modules are staggered in depth by multiples of a tenth of the effective fibre pitch, i.e.  $70 \mu\text{m}$ . The fibres are aligned and glued on a precisely machined support structure made of titanium. Before assembly, the fibres are aluminised to reduce light losses and optical cross-talk. The fibre positions are measured by means of optical metrology



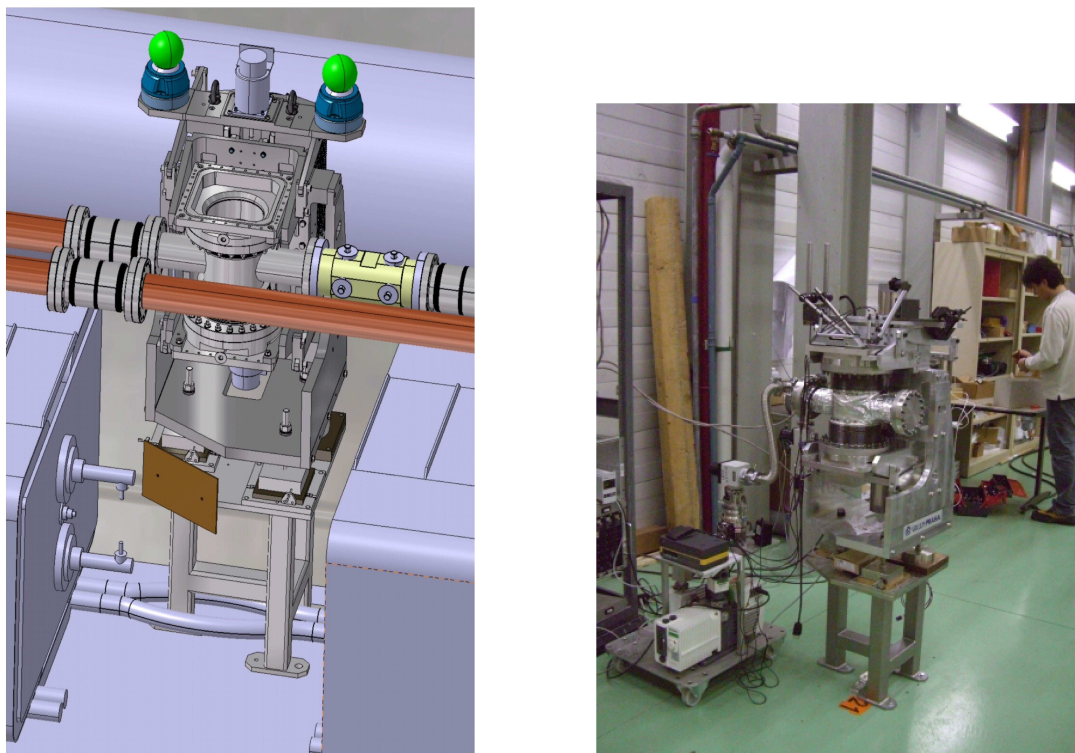


**Figure 7.4:** Schematic view of the support mechanics for one of the ALFA detectors and of its location at a distance of 240 m from the ATLAS interaction point (left). One of the as-built structures, which will house the scintillating-fibre trackers (right).

at various stages of the manufacturing, resulting in a set of equations describing the location of each fibre in a given detector.

The overall layout with the front-end electronics is shown in figure 7.5. The module support structure is connected to a base-plate, which is mounted on the Roman-pot flange. The base-plates also house optical feed-through connectors coupling the fibres to the pixels of multi-anode phototubes. The multi-anode phototubes with 64 channels are aligned to the fibres and shielded against residual stray magnetic fields. Anode signals from these phototubes are fed into the front-end boards and further processed by the front-end multi-anode readout chips.

To achieve an accurate alignment of the fibre tracker with respect to the centre of the beam, the Roman pots are equipped with special interleaved extrusions, yielding a vertical overlap area when in beam position. These extrusions are instrumented with three layers of vertically staggered overlap detectors consisting of 30 horizontally oriented fibres in each layer. The overlap detectors use the same type of fibres and are read out in the same way as the other detectors.

The central area is further instrumented with two optically separated trigger scintillator tiles providing a fast L1 trigger signal. Single trigger tiles are used in each of the overlap extrusions. The trigger tiles are coupled to clear light-guide fibres routed to standard PMT's with 8 mm diameter. The PMT signals are amplified and processed before being sent to the central trigger processor (see section 8.2.3).

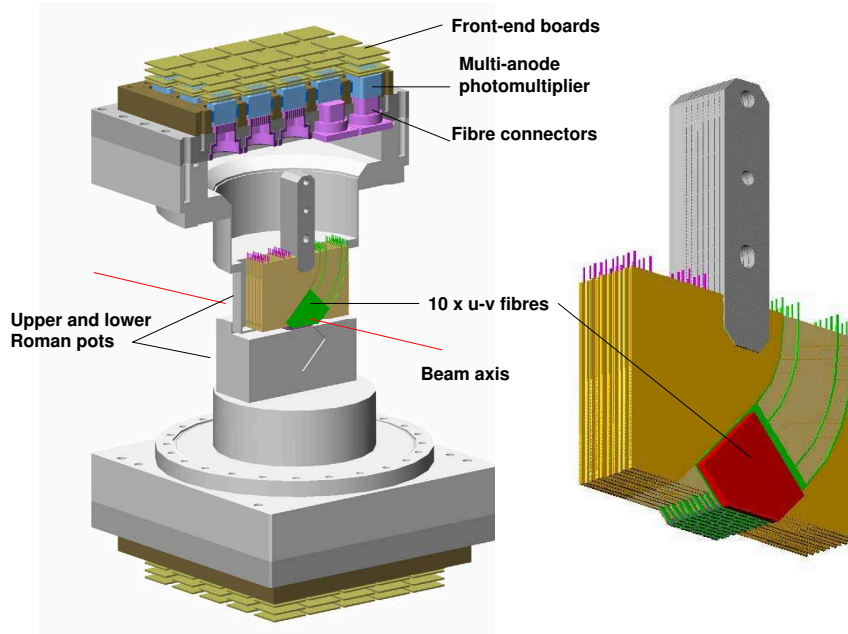


**Figure 7.5:** Schematic layout of the ALFA detector in the Roman pot, showing the scintillating-fibre stack, the fibre connectors, the multi-anode photomultipliers, and the front-end boards. The Roman pots (labelled as upper and lower) approach the beam-line from above and below (left). Details of the scintillating-fibre stack (right).

### 7.2.1 Experimental results from test-beam

Two test-beam campaigns were carried out for the ALFA detectors; the first one at DESY [223] to validate the detector design, and the second one at CERN [224] to test the overlap, trigger, and electronics concepts. Prototypes with ten modules but only a fraction of nominal fibres per module were built and exposed to the beam. The test-beam facilities were partly equipped with high-precision silicon-strip detectors for precise resolution studies. The photoelectric yield of the scintillating fibres was extracted from charge-amplitude measurements of the multi-anode phototubes. The charge response of the multi-anode phototube to single photons was calibrated using a pulsed blue LED. The average number of photoelectrons was  $4.2 \pm 0.5$ , with a relative cross-talk contribution from adjacent fibres of about 3%.

The spatial detector resolution, obtained after deconvolution of the intrinsic contribution of the silicon reference detector of  $30 \mu\text{m}$ , was determined to be  $36 \mu\text{m}$  in both the  $x$  and  $y$  directions. For the low-energy electron beam used at DESY, a sizable resolution degradation is expected from multiple scattering, as shown in an energy scan in figure 7.6. Using a high-energy hadron beam at CERN, where multiple scattering is irrelevant, a spatial resolution for ALFA of  $25 \pm 3 \mu\text{m}$  was determined, in agreement with GEANT4 [220] Monte-Carlo expectations.



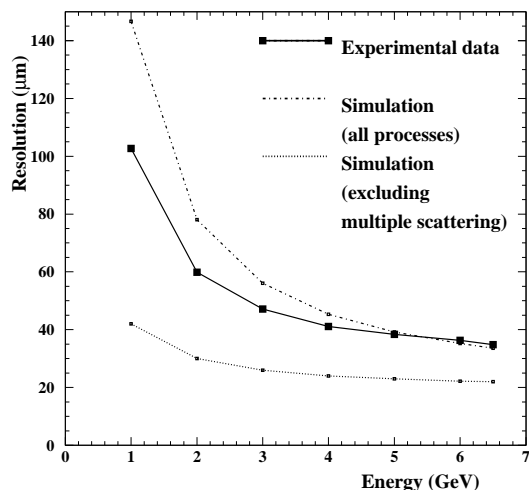


**Figure 7.6:** The spatial resolution as function of the beam energy compared to GEANT4 simulations with and without the contributions from multiple scattering.

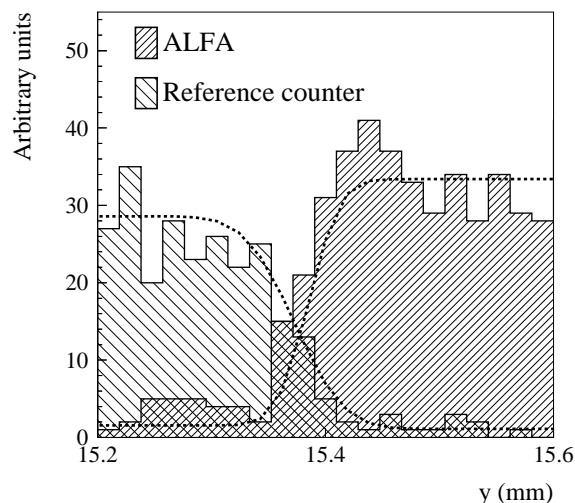


**Figure 7.7:** Comparison between the edges of ALFA and a reference trigger counter of the  $y$  coordinates measured with the silicon detector. Dotted lines represent edge fits smeared by detector resolution for 6 GeV electrons.

The sensitivity of ALFA at the edge closest to the beam, which is essential to cover the required phase-space for the measurements, was studied with an additional scintillator touching the fibres and defining the physical edge. Coordinates of tracks passing either through ALFA or the scintillator were recorded with the silicon detector and fit by edge functions, smeared for spatial resolution effects. As shown in figure 7.7, the edge functions cross very close to the physical ALFA edge and no insensitive region was found. The fitted smearing is consistent with the spatial resolution of the silicon detector. All measured performance parameters were thus found to fulfil the ATLAS requirements [213].

## 7.2.2 ALFA installation in ATLAS

The Roman pots (without detectors) with their precision support mechanics will be produced at the beginning of 2008 and the installation will take place when the LHC schedule will allow it. The ALFA detector itself is still at the prototype stage. A prototype, representing a complete detector for one Roman pot (1/8 of the full system) is under construction. After validation, the series production for the entire system will begin in 2008, aiming for final installation and first measurements in 2009.

## 7.3 The zero-degree calorimeters

The primary purpose of the ATLAS Zero-Degree Calorimeters (ZDC) [213] is to detect forward neutrons with  $|\eta| > 8.3$  in heavy-ion collisions. The ZDC's play a key role in determining the centrality of such collisions, which is strongly correlated to the number of very forward (spectator) neutrons. During the start-up phase of the LHC ( $p$ - $p$  collisions with luminosities well be-

low  $10^{33} \text{ cm}^{-2} \text{ s}^{-1}$ ), the ZDC's will enhance the acceptance of ATLAS central and forward detectors for diffractive processes and provide an additional minimum-bias trigger for ATLAS.

Significant backgrounds in hadron-collider experiments are created by beam-gas and beam-halo effects. These can be greatly reduced by requiring a tight coincidence from the two arms of the ZDC's, located symmetrically with respect to the interaction point. For  $p$ - $p$  scattering, this coincidence, as determined from PYTHIA [225] simulations, is found to be 9% of the total inelastic rate and will therefore be important for initial beam tuning at the beginning of LHC operation. The time resolution of the ZDC's is roughly 100 ps, which is sufficient to locate the interaction point to about 3 cm in  $z$  (along the beam axis). This would therefore provide some knowledge of the vertex location without using the inner detector information.

The ZDC's reside in a slot in the TAN (Target Absorber Neutral) absorber, which would otherwise contain inert copper bars as shielding. The TAN is located at  $\pm 140$  m from the interaction point, at the place where the straight-section of the beam-pipe is divided back into two independent beam-pipes.

### 7.3.1 ZDC module description

There will be four ZDC modules installed per arm: one electromagnetic (EM) module (about 29 radiation lengths,  $X_0$ , deep) and 3 hadronic modules (each about 1.14 interaction lengths,  $\lambda$ , deep).

Table 7.1 summarises the mechanical properties of the ZDC system. The EM module of one arm is shown in figure 7.8a). It consists of 11 tungsten plates, with their faces perpendicular to the beam direction. The height of these plates is extended in the vertical direction with 290 mm long steel plates. A total of 96 quartz rods of 1.0 mm diameter penetrate the tungsten plates parallel to the beam in a  $8 \times 12$  matrix, which is transverse to the beam. Along the face of the module the rods are bent upwards at an angle of  $90^\circ$  and are viewed by multi-anode phototubes capturing the Cerenkov light from shower products of incident particles. The position of the rods containing a signal thus corresponds to the position of the incident particle transverse to the beam, and the intensity of the light reflects the energy of the particle. Only one of the arms, at  $-140$  m, is equipped with the position-sensing capability for its EM module.

Between the tungsten and steel plates are placed 1.5 mm quartz strips which are routed vertically and are viewed from above by photomultiplier tubes via air light-guides. These strips are actually rows of quartz rods called strips, in order to distinguish them from the position-measuring rods. These strips are depicted in figure 7.8b). The purpose of the strips is to obtain a second, improved measurement of the incident particle energy. In the position-sensing EM module there are four such light-guides, side by side, since more than one incident particle per event is expected.

The hadronic modules are similar, but while the EM module maps the 96 position-measuring rods each onto one pixel of the multi-anode phototube, the hadronic modules map clusters of four rods into individual phototubes and have only one light-guide. Not all hadronic modules have position-sensing rods (there is only one position-sensing module per arm).

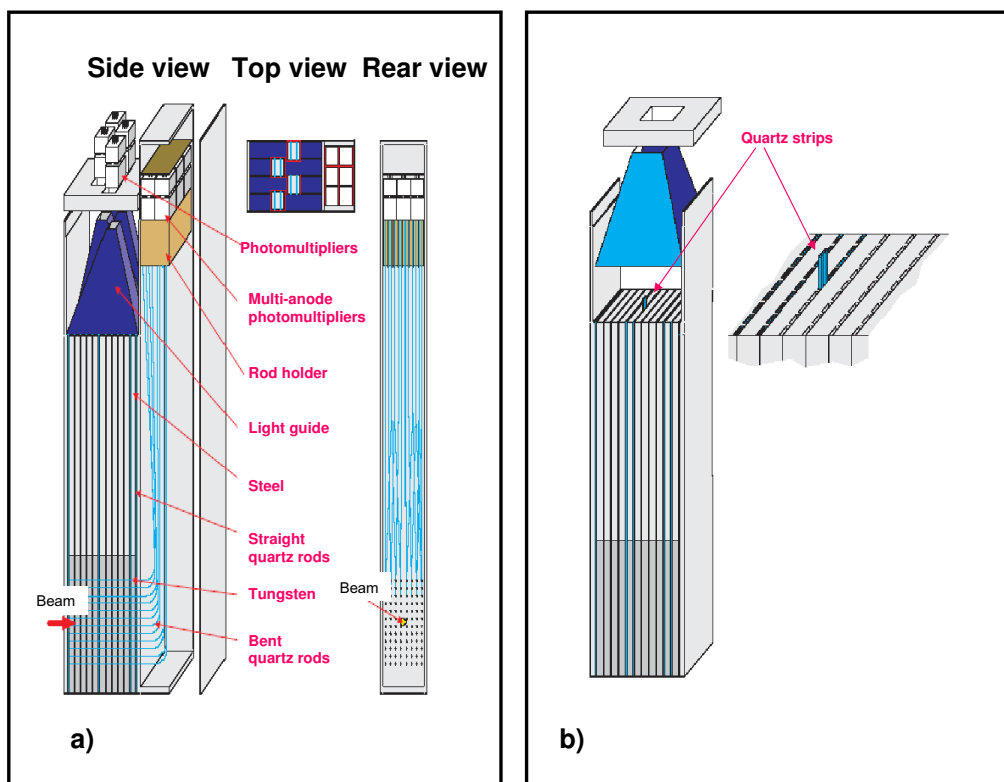


**Figure 7.8:** a) The electromagnetic ZDC module. The incident particles impinge on tungsten plates at the bottom of the module and produces showers of particles. The quartz rods pick up the Cerenkov light generated by the shower and transmit it to multi-anode phototubes at the top of the module. The phototubes measure light from the quartz strips through four air light-guides. b) Details showing the placement of the quartz strips.

## 7.3.2 Calibration and monitoring

### 7.3.2.1 Flashers

Measurements over long periods of time and limited access to the tunnel require that the PMT gains be remotely monitored to an accuracy of about 1%. This can be achieved with a system based on blue LED's. A controllable generator located in the underground side-cavern USA15 will excite the LED in the tunnel. Each PMT will view a fibre connected to the LED, and one fibre will illuminate each large single channel PMT.

The LED is mounted opposite a pin-diode which tracks its stability. Around the pin-diode are eight primary optical fibres. Light in these fibres will travel 5 m to the modules. The light from three of these primary fibres is split further into eight secondary fibres. Light from each of these secondary fibres impinges on each of the 24 phototubes in the hadronic position-sensing module. Four more of the eight primary fibres will calibrate the phototubes in the hadronic position-sensing and energy-measuring modules. The eighth primary fibre is a spare.

The LED monitoring system is not subjected to the large doses of radiation seen in the ZDC's and so deterioration of the system due to radiation damage is not expected.

**Table 7.1:** Summary of ZDC mechanical properties.

	Electromagnetic (at $-140$ m)	Electromagnetic (at $+140$ m)	Hadronic (per arm)
Number of modules	1	1	3
Number of position-sensing modules	1	none	1
Number of energy-measuring light-guides	4	1	3
Total depth	$29 X_0$	$29 X_0$	$4.6 \lambda$ (includes EM module)
Module size (mm):			
width	93.8	93.8	93.8
height	738	738	738
depth	150	150	150
Number of plates/module	11	11	11
Tungsten plate size (mm):			
width	91.4	91.4	91.4
height	180	180	180
depth	10	10	10
Module weight (kg)	80	80	80
Number of 1.5 mm quartz strips	648	648	648
Number of 1 mm pixel rods	96	none	96
Number of pixel readout channels	96	none	24

### 7.3.2.2 Particles

Full calibration of the ZDC detector begins with the determination of the gains in all rod/phototube chains, and continues with the measurement of shower-shape distribution functions, such as the dependence of single-rod amplitudes on the distance to the shower centre. These parameters will be permanently monitored during operation. This preliminary calibration is followed by one using  $\pi^0$  decays in situ in  $p$ - $p$  collisions. During heavy-ion operations, peripheral ion collisions will yield samples of mono-energetic neutrons with the beam energy of 2.75 TeV, providing a useful redundancy check of the calibration constants.

### 7.3.3 ZDC installation in ATLAS

The ZDC is being installed in two stages because it shares the TAN location with the LHCf detector [226]. The LHCf experiment will run during early 43-bunch operation of the LHC and will then be removed. Since the LHCf detector occupies the space of the first ZDC module in each arm, only the three downstream modules in each arm will be installed during this phase. The full ZDC will be in place for the luminosity ramp-up of the machine beyond 2008. As soon as the LHC reaches luminosities above  $10^{33} \text{ cm}^{-2} \text{ s}^{-1}$ , the ZDC modules will be removed for  $p$ - $p$  operation and reinstalled only for the heavy-ion periods. This will be necessary in order to minimise radiation damage to the quartz radiator in the ZDC.